Landsc Ecol (2026) 41:126
https://doi.org/10.1007/s10980-026-02372-5

RESEARCH ARTICLE

Check for updates

A workflow to optimize spatial sampling in ecoacoustic studies

Víctor M. Martínez-Arias · Carolina Paniagua-Villada · Maria José Guerrero · Juan Manuel Daza

Received: 24 July 2025 / Accepted: 1 May 2026 / Published online: 23 May 2026

Abstract
Context Landscape monitoring through sounds relies on spatial sampling to characterize soundscape variation across a heterogeneous space. This non-invasive approach complements traditional landscape metrics by capturing ecological dynamics not visible in spatial structure alone. However, the effectiveness of different spatial sampling strategies remains poorly understood.

Objectives We examined how spatial sampling design affects the representativeness of soundscape information across heterogeneous ecosystems. Our main objective was to identify efficient spatial sub-sampling strategies in ecoacoustics that capture landscape heterogeneity while balancing sampling effort and effectiveness. Specifically, we (1) assessed how sampling structure and effort affect interpolated soundscape representativeness; (2) compared random, thematic designs based on land-cover classes, and tessellation-based designs; (3) examined interactions among landscape, acoustic, and temporal variables; (4) evaluated the influence of landscape heterogeneity on sampling performance; and (5) developed a workflow to guide spatial sub-sampling for ecoacoustics.

Methods Our study was conducted across three Colombian ecosystems. We constructed discrete and continuous landscape proxies using Sentinel-2 imagery, calculated acoustic indices from field recordings, and then implemented various spatial sampling designs from sub-samples based on image tessellation techniques. Using kriging, a geostatistical method for interpolation, we compared sub-samples to full spatial scenarios and assessed their performance using structural and distributional metrics. We took representativeness as the spatial fidelity of interpolated soundscape surfaces relative to full sampling, capturing both acoustic patterns and underlying landscape structure.

Results We found that tessellation-based methods, especially those based on watershed segmentation,

Supplementary Information The online version contains supplementary material available at https://doi.org/10.1007/s10980-026-02372-5.

V. M. Martínez-Arias (✉) · C. Paniagua-Villada · J. M. Daza
Grupo Herpetológico de Antioquia GHA, Instituto de Biología, Facultad de Ciencias Exactas y Naturales, Universidad de Antioquia UdeA, Calle 70 No. 52-21, Medellín, Colombia
e-mail: vmanuel.martinez@udea.edu.co

J. M. Daza
e-mail: juanm.daza@udea.edu.co

V. M. Martínez-Arias · C. Paniagua-Villada
Corporación Merceditas, Calle 3 29A-11, casa 110, Medellín, Colombia

V. M. Martínez-Arias
Fundación Cunaguaro, Yopal, 850001, Casanare, Colombia

M. J. Guerrero
SISTEMIC, Facultad de Ingeniería, Universidad de Antioquia UdeA, Calle 70 No. 52-21, Medellín, Colombia

significantly outperformed random and thematic designs, showing higher sample performance, stronger correlations with sample size, and greater representativeness of landscape heterogeneity. Multivariate analyses showed that tessellation-based designs exhibited consistent patterns across acoustic, temporal, and landscape variables. Our results demonstrate that the spatial arrangement of sampling locations, rather than sample size alone, critically determines sampling performance. We propose a landscape-based workflow to support the design of efficient spatial sampling strategies for ecoacoustics. This approach advances scalable and spatially informed biodiversity monitoring using ecoacoustics methods.

Keywords Soundscape representativeness · Landscape heterogeneity · Passive acoustic monitoring (PAM) · Remote sensing · Landscape segmentation

Introduction

Ecoacoustic research, the study of relationships between living organisms and their environment through sound, has emerged as a powerful and non-invasive approach for monitoring biodiversity and environmental change. By analyzing soundscape patterns, ecoacoustics provides scalable insights into ecosystem dynamics (Gibb et al. 2019; Farina and Li 2022; Farina et al. 2023). Data from acoustic monitoring can be linked to several ecological parameters, including species occurrence, distribution, and richness, community composition, and ecosystem dynamics (Alcocer et al. 2022). This information offers a window into behavioral interactions and ecological processes that often go unnoticed, and are a core assumption in ecoacoustic research: that acoustic data reflect both biotic activity and the underlying landscape structure (Gibb et al. 2019; Alcocer et al. 2022; Rendon et al. 2022).

Several studies have shown that soundscape patterns are related to landscape composition and configuration, highlighting their spatial correspondence with landscape structure (Fuller et al. 2015; Scarpelli et al. 2021; Guerrero et al. 2025; Rendon et al. 2025). Since acoustic data reflect both biotic activity and landscape structure, ecoacoustics is inherently dependent on spatial dynamics. This makes spatial sampling a critical component of study design, ensuring data quality and ecological representativeness. However, many ecoacoustic studies still rely on convenience-based or random sampling approaches, which may fail to capture the spatial complexity of heterogeneous environments. As the demand for reliable, scalable soundscape monitoring grows, there is a pressing need to revisit how spatial sampling design affects the integrity of ecoacoustic inference. In this context, sampling designs may vary according to how they incorporate landscape information (e.g. land-cover classes or continuous environmental gradients), temporal structure (e.g. daily activity periods), and acoustic descriptors (e.g. indices summarizing soundscape properties across frequency bands).

Despite the relevance of sampling design in ecoacoustics, little is known about how specific spatial sampling choices affect the representativeness of soundscape information. Sampling design has been consistently acknowledged as a methodological gap in the field (Sugai et al. 2019; Abrahams et al. 2021; Ross et al. 2023). However, most studies to date have focused on acoustic indices parameters or ecological interpretation, rather than on how spatial sampling choices influence the representativeness of soundscape patterns (Farina et al. 2024; Bradfer-Lawrence et al. 2025; Kemp et al. 2025). This gap remains, even with the increasing availability of remote sensing data, spatial tools, and statistical methods from landscape ecology that could inform pre-field planning (Kerr and Ostrovsky 2003; Hong et al. 2004; Radoux et al. 2019). It is still unclear whether spatially adaptive strategies, i.e. sampling designs that adjust devices location according to landscape structure, such as segmentation or gradient-based subdivision, offer tangible advantages over random or thematic (e.g. landcover type) approaches, especially in structurally complex environments.

To address this gap, we ask: How does spatial sampling design influence the performance and representativeness of soundscape information in ecoacoustic studies across heterogeneous landscapes? Our main objective was to identify efficient strategies for spatial sub-sampling in ecoacoustics that account for landscape heterogeneity while balancing sampling effort and effectiveness. Specifically, we: (1) analyzed how sampling structure and sample size affect the representativeness. Here, we use the term representativeness to refer to how well a given sampling design captures the spatial structure of soundscape patterns emerging from both acoustic activity and underlying landscape heterogeneity; (2) compared the performance of random, thematic designs based on land-cover classes, and tessellation-based designs, including those derived from segmentation methods; (3) explored how landscape, temporal, and acoustic variables interact to shape the multivariate structure of Sub-sampling outcome. In this context, landscape variables reflect both composition (land-cover classes) and continuous spectral gradients, temporal variables correspond to distinct daily periods (full day, dawn, evening), and acoustic variables represent indices summarizing soundscape properties across multiple frequency bands; (4) assessed the influence of landscape heterogeneity on sampling performance; and (5) developed a methodological workflow to guide spatial sampling choices in future ecoacoustic monitoring efforts.

In this study, we address these objectives using multiple frequency ranges and time periods, recognizing that acoustic activity is structured along frequency and time as a consequence of taxonomic composition, behavioral patterns and environmental filtering. Testing sampling strategies across contrasting spectral windows and biologically meaningful time blocks allows us to evaluate the robustness of spatial representativeness across different acoustic configurations shaped by landscape heterogeneity.

Methods

To analyze the effects of landscape heterogeneity on sampling designs in soundscape studies, we selected three study localities with different degrees of heterogeneity (see "Study sites and recorder deployment" section). Next, we determined recorder placement sites, collected audio recordings, and used their location data to generate bounding boxes for modeling procedures. Within these bounding boxes, we extracted discrete and continuous landscape proxies (see "Landscape proxies" section and Supplementary Information S1) and calculated acoustic indices to quantify the soundscapes (see "Soundscape calculation" section and Supplementary Information S2).

To evaluate different sampling designs, we used landscape proxies as criteria to construct Sub-sampling scenarios from an initial design, which included all our available recorders (see "Sub-samples generation" section and Supplementary Information S3). In addition, we created random sub-samples for each initial design (see "Sub-samples generation" section). We then interpolated the acoustic indices for both the full recorder design and its corresponding sub-samples (see "Spatial interpolation of acoustic indices" section and Supplementary Information S4). To develop our research question and the first four specific objectives we applied correlation metrics, non-parametric statistics, and multivariate analysis to evaluate sampling effectiveness, robustness, and landscape representativeness (see "Data analyses" section and Supplementary Information S5–S8).

Study sites and recorder deployment

We selected three study localities aiming to represent the heterogeneity of Colombian ecosystems, based on landcover composition, terrain variation, and land use (Milne 1991; Ali et al. 2014). The first locality is in an urban Andean area, featuring an urbanization gradient that is inversely correlated with elevation. The second locality is in a rural Andean zone, encompassing a gradient of agricultural uses ranging from pastures to forest cover, over highly rugged terrain. The third locality is in the Colombian plains, in a zone characterized by a combination of natural savanna and riparian forests, used for both cattle grazing and conservation, over predominantly flat terrain (Fig. 1).

After selecting the study localities, we determined the sites for installing AudioMoth© recorders (versions 1.0, 1.1 and 1.2). In the Rural Andean (45 recorders) and Colombian Plains localities (96 recorders), we implemented a grid design, placing recorders 400 m apart to ensure data independence in a homogeneous way (Metcalf et al. 2023). Logistical constraints prevented us from implementing homogeneous design in the Urban locality (55 recorders), however, we maintained the same 400 m spacing between recorders (Fig. 1). Each recorder was configured to record 1 min every 15, at a sampling rate of 194,000 Hz between 7 and 10 days, with a med–high gain (4/5 in AudioMoth configuration). Prior to field

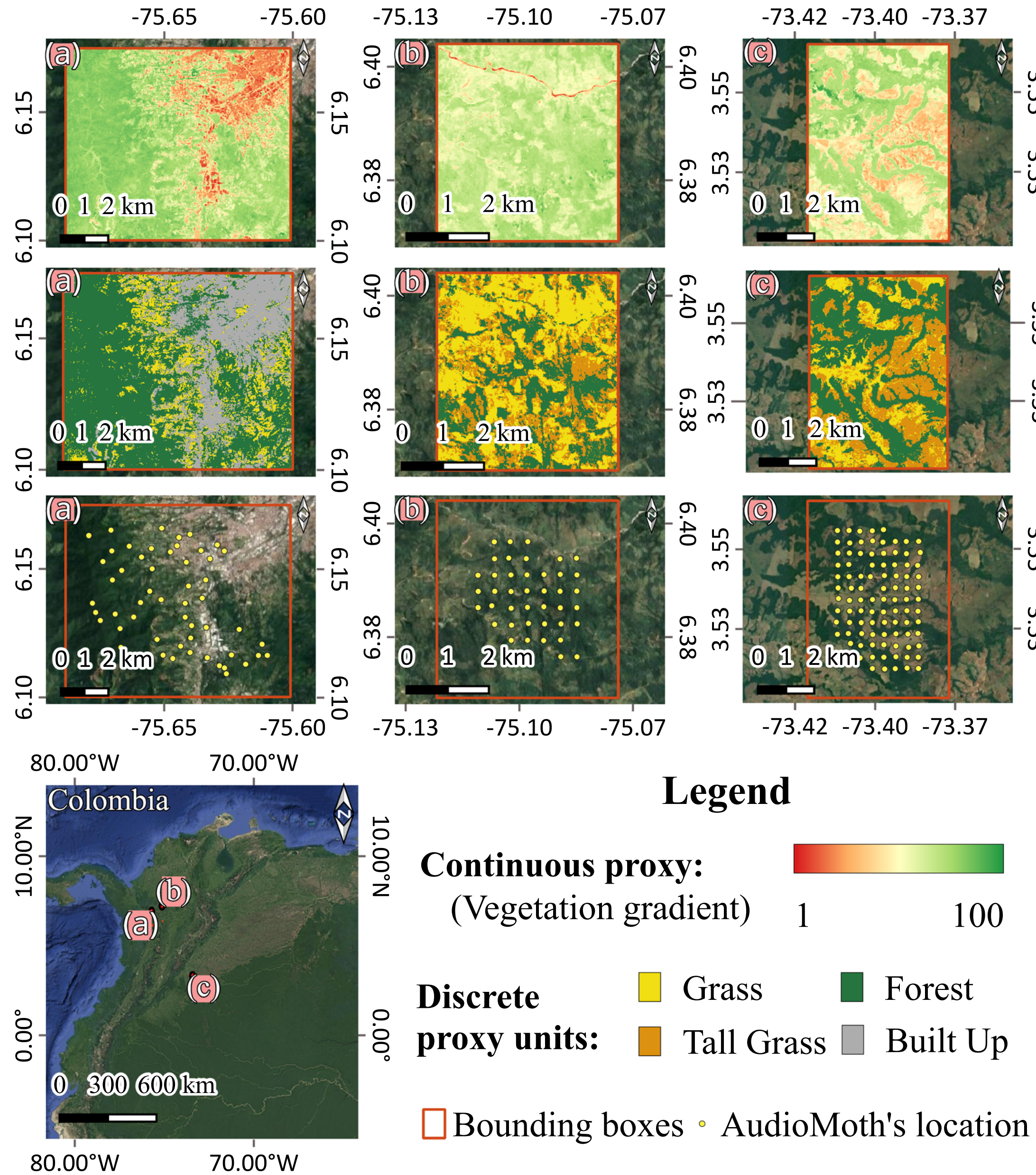

ID.	Locality	Municipality	Elevation range	Recorders
(a)	Urban Andean	La Estrella (Antioquia)	1700-3000	55
(b)	Rural Andean	Alejandría (Antioquia)	1400-1900	45
(c)	Colombian Plains	San Martín (Meta)	200-300	96

◂**Fig. 1** Study sites, landcover types, and sampling grid layouts across three Colombian landscapes. The figure includes each full grid deployed recorders arrangement. Panels **a** to **c** in the top row show the continuous landscape proxy based on a vegetation gradient (scaled from 1 to 100), derived via PCA from NDVI, SLAVI, and MNDWI spectral indices. Panels **a** to **c** in the middle row depict the discrete landscape proxy, obtained through random forest classification into four landcover types: Grass, Tall Grass, Forest, and Built-up areas. Panels **a** to **c** in the bottom row display the distribution of sampling points (yellow dots) within the predefined bounding boxes (red outlines) for each locality: **a** Urban Andean, **b** Rural Andean, and **c** Colombian Plains. The bottom-left map shows the geographic location of the study sites across Colombia. The accompanying table summarizes the locality names, municipalities, and elevation ranges for each study area. Versions of each AudioMoth recorder and date of deployment can be found both in Supplementary Information S12 on each site' corresponding UDAS file, and in each geojson file starting with "Points_", in the QGIS project from the Supplementary Information S13. Basemap: Google Satellite/Hybrid imagery, Mapdata ©2026 Google

deployment, recorder gain consistency was verified using a power spectral density-based test signal procedure to ensure comparable recording sensitivity across devices. This verification step was performed exclusively for pre-deployment quality control; no post hoc gain correction or signal normalization was applied to the recordings.

All deployment metadata associated with this study were compiled into a structured summary table referred to as the Unified Database for Acoustic Surveys (UDAS). UDAS is an Excel-based table that integrates recorder specifications, spatial location, deployment dates, deployment duration, recording schedule, and habitat descriptors for each sampling site, accompanied by a vocabulary sheet documenting variable definitions and units. Each locality-specific UDAS file is provided in Supplementary Information S12.

Using the recorders coordinates, we generated locality-specific bounding boxes expanded by 1 km in all four cardinal directions. These generated bounding boxes were used as modelling areas for soundscape proxy construction, and for landscape proxy construction. We used rectangular bounding boxes as modeling extents for computational efficiency and reproducibility in Google Earth Engine, without affecting the effective area of analysis defined by recorder locations and their buffered zones of influence; preliminary tests showed that irregular or circular geometries substantially increased processing time. Figure 1 provides a visual summary of the study regions, including the geographic location of each site, the layout of sampling grids, and the landscape proxies used in subsequent analyses.

Landscape proxies

We used Google Earth Engine to gather Sentinel-2A images for each study area, applying a 10% cloud filter and generating NDVI-based best-pixel mosaics (Gorelick et al. 2017; Google Earth Engine 2023a). From these mosaics, we derived two landscape proxies based on the concept of ecotope as the minimum spatial unit of landscape (Radoux et al. 2019; Farina 2022; Francis et al. 2022). The first was a continuous proxy via PCA on scaled spectral indices (Normalized Difference Vegetation Index—NDVI, Specific Leaf Area Vegetation Index—SLAVI, Modified Normalized Difference Water Index—MNDWI), reflecting vegetation, structure, and water presence (Kriegler et al. 1969; Lymburner et al. 2000; Xu 2006; Abdi and Williams 2010; Mishra et al. 2014). The resulting PCA fusion was scaled from 1 to 100, where 1 corresponds to bare and built-up areas (low leaf area, constructions) and 100 represents highly vegetated environments (dense canopy). In this proxy, ecotopes are pixel-based, with each pixel representing a uniform spatial unit of analysis.

The second was a discrete proxy via random forest classification into four landcover types: Forest, Built-up, Grass, and Tall Grass. Classification accuracy was optimized to ~ 80% using confusion matrices (Cansler and McKenzie 2012; Hejmanowska et al. 2021; Google Earth Engine 2023b). In this case, ecotopes correspond to spatially explicit landcover patches, which may vary in size and shape. Detailed methods for the construction of each proxy are provided in Supplementary Information S1.

Soundscape calculation

Soundscape proxies were generated by processing recordings using Power Spectrum Density (PSD) between 600 and 1200 Hz via Welch's method to exclude corrupted and rain-affected files (Bedoya et al. 2017). From the cleaned recordings, we computed the following acoustic indices: Acoustic Complexity Index calculated in its temporal (ACItf) and spectral (ACIft) formulations, Number of Peaks

(NP), Bioacoustic Index (BI), and the Normalized Differenced Soundscape Index (NDSI) to capture soundscape complexity across spectrogram, spectrum, and signal characteristics (Sánchez-Giraldo et al. 2021; Luna-Naranjo et al. 2024). These selected indices support analyses of biotic activity and anthropogenic disturbance (Boelman et al. 2007; Kasten et al. 2012; Alcocer et al. 2022; Farina and Li 2022).

Since acoustic activity is structured along frequency and time as a consequence of taxonomic composition, behavioral patterns, and environmental filtering, we computed NP, ACItf and ACIft across three frequency bands (0–24, 0–12, 12–24 kHz). In the case of BI and NDSI, we used these indices' standard frequency ranges (BI 2–12 kHz; NDSI 0–2 kHz) to preserve their established ecological interpretation. Additionally, we calculated all indices within three daily periods: full day, and dawn (05:00–08:00) and evening (17:00–20:00), according to Rendon et al. (2025). For ultrasonic recordings, we computed NP, ACItf, ACIft, and BI within the 25–96 kHz frequency range, for methodological consistency, we used the same temporal subdivision as in the audible domain (full day, dawn, and evening).

For ACI's calculations, differential spectral representations were used depending on the frequency domain. In the audible range, ACI was computed from power spectrograms to maximize energetic contrasts and to evaluate sampling strategies under conservative and high-contrast conditions. However, for ultrasonic frequencies, ACI's were calculated from amplitude spectrograms with edge-effect correction, following Farina and Li (2022), in order to avoid artificial amplification of variability and false positives in low-energy, high-frequency signals. Detailed methods for the calculation of the acoustic indices using the scikit-maad package for python (Ulloa et al. 2021) are provided in Supplementary Information S2. Python codes are also provided in Supplementary Information S14.

For clarity, acoustic indices were not combined at any point in the workflow. Each index (ACItf, ACIft, BI, NDSI) was calculated independently for every recorder, frequency band, and, where applicable, time period. Because each site generated multiple recordings within each period, we summarized temporal variation by computing the median value of each index per recorder, per time period, and per frequency band. These median values represent independent soundscape proxies and were used separately in further data processing (i.e. interpolations).

Sub-samples generation

We implemented Sub-sampling using random and stratified designs across a full set of initial recorder locations. Random sub-samples included 20%, 40%, 60%, and 80% of the full set, iterated 50 times.

We based the stratified approaches on four landscape segmentations (see Supplementary Information S1 and S3 for further details): (1) land-cover classes representing discrete proxies; (2) Superpixels Linear Iterative Clustering (SLIC), which segments an image into visually homogeneous regions (Achanta et al. 2012); and watershed-derived (3) Basins and (4) Halfbasins, which partition continuous landscape proxies into spatially coherent units based on underlying gradients (Fig. 2; Palomino and Hilares, 2011). The tile area (A_i) for SLIC and watershed-derived tessellations procedure was defined as the area of a circle with radius = 200 m, which we used as a spatial independence radius rather than as an estimate of biological detection range. This distance was selected to minimize spatial overlap and maintain independence among recording sites, following recommendations from spatial ecoacoustic assessments (e.g., Bicudo et al. 2023). The resulting area, used purely as a geometric constraint to guide the scale of tessellation units, is:

$$A_i = \pi r^2 = \pi (200\,\mathrm{m})^2 = 125.664\,\mathrm{m}^2 \approx 0.126\mathrm{k}\,\mathrm{m}^2.$$

After generating all tessellations, we proceeded with Sub-sampling by selecting representative points within each unit. To do so, we identified the pole of inaccessibility within each of the generated tiles for each tessellation (Landcover, SLIC, Basins, Halfbasins) using the Shapely library (Gillies 2013). We then selected the sample point nearest to each pole of inaccessibility from the original recorder grid in each bounding box (Fig. 2). Importantly, all sub-sampling procedures were strictly spatial: whenever a recorder location was included, all its recordings were retained. Temporal (daily periods) and spectral subsets were introduced later during index calculation, identically for all designs. Therefore,

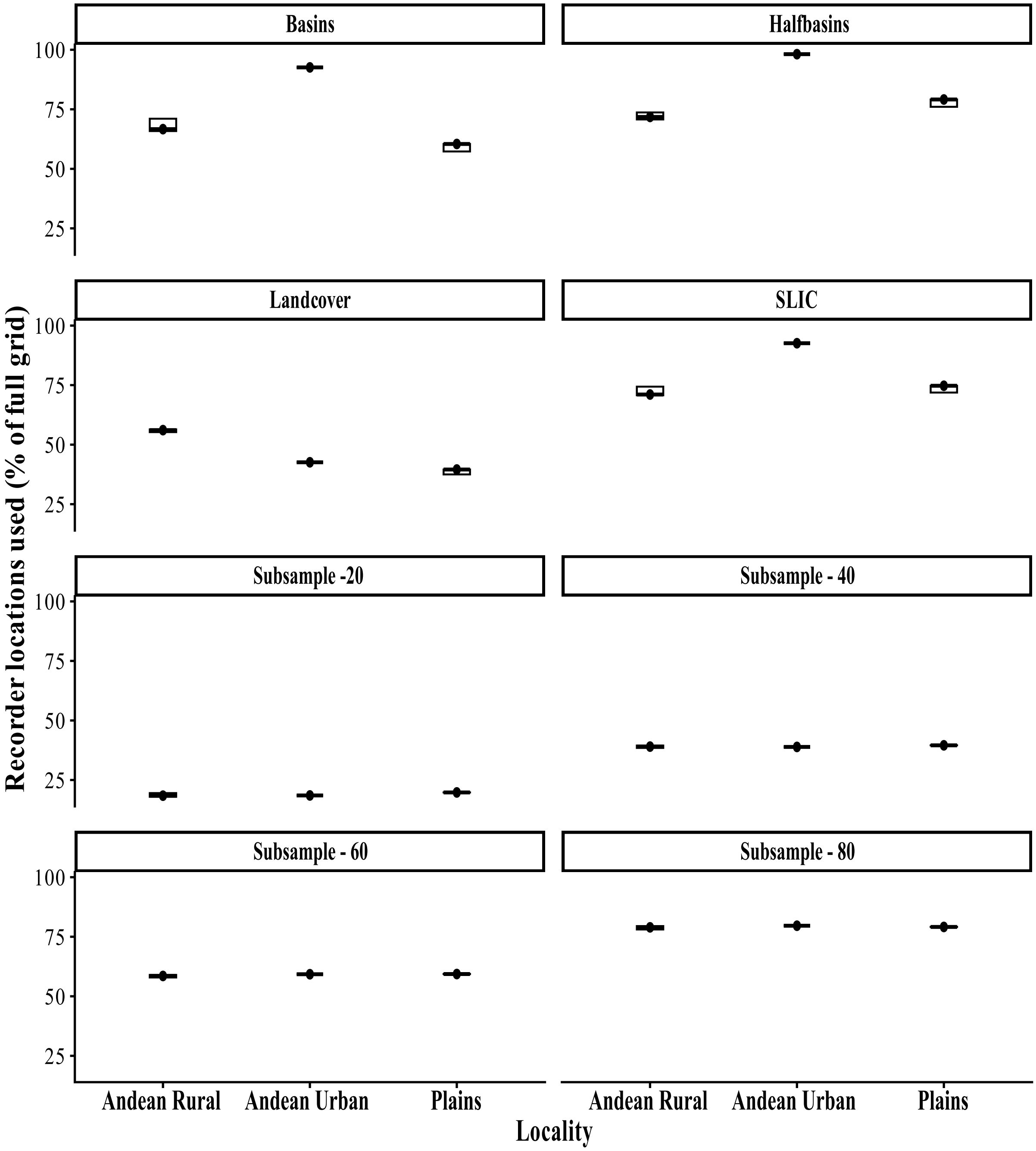

Fig. 2 Proportion of recorder locations retained under each sub-sampling strategy across the three study localities. Each panel corresponds to a sub-sampling strategy (Basins, Halfbasins, Landcover, SLIC, and random sub-samples at 20%, 40%, 60%, and 80%). For each locality, values represent the percentage of recorder locations retained relative to the full sampling grid. Boxes indicate the interquartile range, horizontal lines represent the median, and points show the central tendency across realizations. Minor variation around nominal sub-sampling levels (e.g., 20%, 40%) arises from quality-control filtering of recordings and subsequent subdivision into daily periods during index calculation; these differences are negligible and do not reflect changes in the spatial sampling design. The figure provides a standardized comparison of sampling effort across strategies and localities

differences among sub-samples reflect only spatial configuration rather than variation in temporal data.

To document the sampling effort associated with each sub-sampling design, we quantified the proportion of recorder locations retained relative to the full sampling grid at each locality (Fig. 2). Minor differences in the effective proportion of retained locations arise from quality-control filtering of recordings and from subsequent subdivision into daily periods during acoustic index calculation; these differences are negligible and do not reflect changes in the spatial sampling design (Supplementary Information S5).

Spatial interpolation of acoustic indices

We used kriging interpolation to generate spatial soundscape surfaces from the full and sub-sampled grids, applying it to the median value of each acoustic index computed for each recorder location and each combination of frequency band and temporal window (Fig. 2). Kriging accounts for spatial auto correlation and enables evaluation of how well each sampling design captures spatial structure (Zarco-Perello and Simões 2017; Amelia et al. 2023). We estimated the variogram nugget (microscale variation) and sill (total variance) empirically for each index and dataset, but used a fixed theoretical range of 200 m during interpolation to ensure comparability among full and sub-sampled scenarios. This range does not correspond to the pixel size of the output raster (which was 10 m), but rather to the spacing structure imposed on the kriging model. Detailed interpolation settings are provided in Supplementary Information S4.

Data analyses

We took the interpolated surfaces from each sub-sampling scenario and compared them with the corresponding full dataset interpolation on each locality to calculate each sub-sample performance, using the Pearson correlation coefficient (Fortin et al. 1989; Borcard et al. 2011). We selected Pearson's ρ for being easily interpretable and sensitivity to continuous spatial variation. We calculated the correlations using the ArchGDAL package in Julia. Higher correlation values indicate greater spatial fidelity of the sub-sample relative to the full landscape interpolation (Fig. 3).

Evaluation of the sample size influence over sampling design

To evaluate how sample size influences sub-sample performance across varying ecological and methodological conditions, we calculated a second Pearson correlation coefficient (hereafter Pcoeff2) between sampling proportion and sampling performance (as quantified by the spatial Pearson correlation described above in "Data analyses" section). This analysis (Pcoeff2) therefore relates variation in sampling effort to changes in spatial fidelity, rather than comparing spatial values directly.

The Pcoeff2 correlation was computed independently for each combination of locality, Subsampling strategy, frequency range, time period, acoustic index, and summary statistic, yielding a distribution of Pcoeff2 values per strategy. We then evaluated the normality of the distribution of these correlation coefficients (Pcoeff2) within each strategy using the Shapiro–Wilk test (Kassambara 2019). As most distributions were non-normal, we used the Wilcoxon rank-sum test to compare "random" vs. "tessellation" strategies and the Fligner–Killeen test to assess differences in dispersion (Sarkar et al. 1999). See Supplementary Information S5 for further details.

Effectiveness of stratified sampling designs

We evaluated the effectiveness of stratified sampling strategies using two metrics: sub-sample performance and sampling efficiency. Sub-sample performance was previously defined as the Pearson correlation (ρ) between the interpolated surface from each sub-sample and the corresponding full grid. To quantify how well each strategy balances performance and effort, we calculated sampling efficiency as the ratio of performance to sampling proportion (sub-sample performance/% sampled). This approach allowed us to identify designs that not only reproduce spatial patterns effectively, but also do so with fewer sampling units.

For both metrics, we computed summary statistics (mean, median, standard deviation, and coefficient of

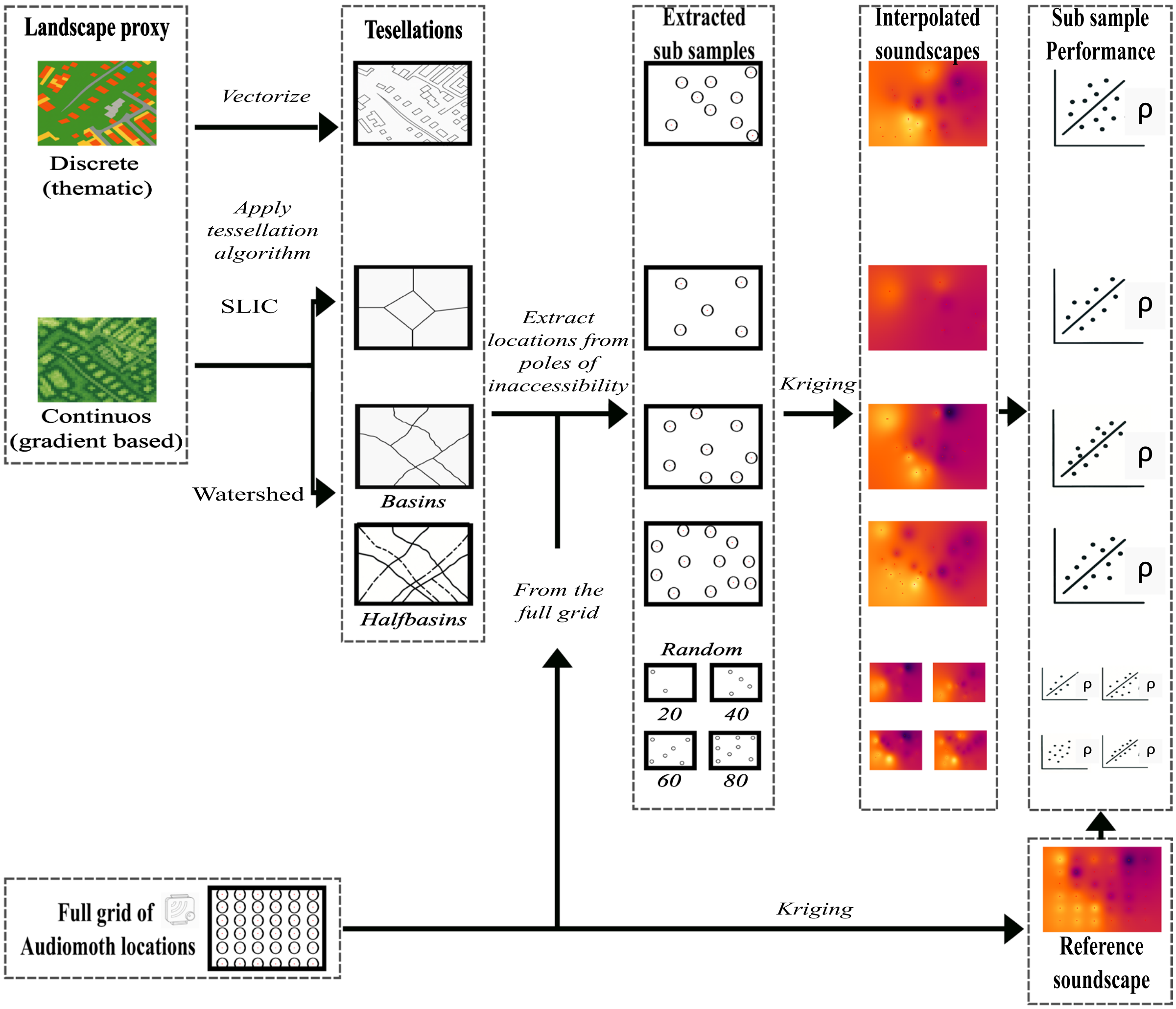

Fig. 3 Pipeline for extracting and evaluating spatial sub-samples based on different arrangements. Discrete and Continuous landscape proxies were tessellated into spatial units using vectorization (landcover), SLIC, and watershed-based methods (Basins and Halfbasins). Sub-sampling locations were selected from the pole of inaccessibility within each tessellation unit, or randomly sampled from the full grid at proportions of 20%, 40%, 60%, and 80%. Each random Sub-sampling level was iterated 50 times to account for variability in selection. Kriging interpolation was applied to each acoustic index to generate soundscape surfaces, and sub-sample performance was quantified by comparing each interpolation to the full grid reference using Pearson correlation (ρ). *Note* the proxy landscapes and interpolated surfaces in this figure were simulated using AI-generated visuals for illustrative purposes only. All analytical procedures, workflows, and spatial arrangements were manually designed by the authors

variation) across all realizations generated for each sample strategy. We did this to capture not only the central tendency of each strategy's performance, but also its variability and reliability across iterations and conditions. This allowed us to assess whether high performance was consistent or driven by outliers, and to identify strategies that offered both effectiveness and robustness.

To determine whether separate subgroup analyses were necessary, we first examined summary statistics for each tessellation strategy across time periods, localities, and frequency ranges. Because performance patterns were broadly consistent across these factors (median Pearson > 0.89, with low to moderate coefficients of variation), we did not subdivide the data further by time period, frequency range, or locality (see Supplementary Information S6). We then evaluated the overall distributions of sub-sample performance and sampling efficiency across strategies. Specifically, we tested normality within each sub-sample group using the Shapiro–Wilk test, visualized the distributions with violin plots overlaid with box plots, and, due to non-normality, compared strategies using Kruskal–Wallis rank-sum tests followed by Dunn's post hoc tests with Benjamini–Hochberg correction for multiple comparisons (Wickham 2011; Wickham et al. 2014; Kassambara 2023; R Core Team 2024; Ogle et al. 2025). See Supplementary Information S6 for further details.

Multivariate structure of stratified Sub-sampling strategies

To evaluate the multivariate structure and the influence of multiple variables in shaping the effectiveness of different stratified sampling designs, we applied a Factorial Analysis of Mixed Data (FAMD). We chose FAMD because it accommodates both categorical (locality, index, sub-sample, frequency range, with sub-sample as supplementary) and continuous variables (sample percent, sub-sample performance) within a single ordination framework. By combining the PCA and the MCA principles, FAMD identifies latent dimensions explaining variance structure (Kassambara 2017).

After performing the FAMD, we found that the first dimension was primarily influenced by performance-related variables (sample percent, sub-sample performance), which are directly related to outcome effectiveness. While Dimension 1 was included in all subsequent statistical comparisons and visualizations, we focused our interpretive attention on Dimensions 2 to 4, as these were more strongly associated with design and landscape characteristics (e.g., index, locality, time_period; see Supplementary Information S3). Finally, we proceed to test differences in latent dimensions across Sub-sampling strategies (Basins, Halfbasins, SLIC, Landcover). To do so, we used Kruskal–Wallis tests per dimension, followed by Dunn's post hoc tests with Benjamini–Hochberg correction (Chen and Sarkar 2020; Ogle et al. 2025). Significance groupings were visualized to clarify which strategies differed structurally across FAMD dimensions for both mean and median statistics. See Supplementary Information S7 for further details.

Stratified sample strategies relation to landscape heterogeneity

To assess how well different tessellation-based Sub-sampling strategies capture landscape heterogeneity, we compared the distribution of the mean landscape proxy between each sub-sample and the complete sampling grid for each locality. Sub-samples were grouped by both tessellation type (e.g., Basins, SLIC, Landcover, Halfbasins) and point source, distinguishing between the poles of inaccessibility identified within each tessellation unit and the nearest original recorder locations selected for sampling. We used kernel density estimates (KDE) and quantile–quantile (Q–Q) plots for visual comparisons (Supplementary Information S8). Statistical similarity was assessed using the Kolmogorov–Smirnov (KS) test to evaluate distributional equivalence, and the Wasserstein distance to quantify shape and displacement differences (Ramdas et al. 2017). The spatial error associated with sampling location was also assessed via the distance to pole, a measure of how far each sampled point was from the centroid of its spatial unit. We compiled all results by locality.

Results

Our results showed that spatial sampling design has a clear and significant influence on the representativeness of ecoacoustic data across heterogeneous landscapes, where performance refers to how well a sub-sample represents the soundscape derived from the full recorder array. Stratified, tessellation-based designs, particularly Basins and Halfbasins, consistently outperformed random sampling, exhibiting stronger correlations with sample size, lower dispersion, and more stable performance–efficiency trade-offs. These designs also showed greater structural coherence in multivariate space and smaller distributional deviations from complete samples. Between the tessellation types, the landcover approaches demonstrated higher variability and spatial error.

Influence of sample size was stronger in tessellation-based than random designs

We found that tessellation-based strategies exhibited a significantly stronger and more consistent correlation between sample size and sampling performance compared to random designs. This was supported by their markedly lower coefficient of variation (CV), which was at least 12 times lower than that of the random strategies (Table 1; Fig. 4; Supplementary Information S5). Furthermore, random sampling designs showed high variability, and thus greater unpredictability, in response to changes in sampling effort (Table 1; Fig. 4). These results were statistically supported by a Wilcoxon rank-sum test ($W = 925$, $p < 0.001$), and a Fligner–Killeen test for homogeneity of variances ($\chi^2 = 10.97$, $p = 0.000926$) for the audible range. In the ultrasound range, although random designs presented higher dispersions, the variance difference was not statistically significant ($\chi^2 = 2.00$, $p = 0.157$).

Watershed-based sampling designs: greater effectiveness than other stratified sampling strategies

We found clear differences in sub-sample performance and sampling efficiency among stratified sampling strategies across both audible and ultrasonic domains (Fig. 5; Table 2; Supplementary Information S6). Specifically, Halfbasins achieved the highest median sub-sample performance in both domains (Audible median Pearson = 0.953; Ultrasound = 0.920) but showed higher variability, particularly in the audible range (CV of efficiency = 0.33). In

Table 1 Summary statistics and dispersion measures of the correlation between sample size and sub-sample performance (Pcoeff2) across random and tessellation-based designs, separated by frequency range

Frequency	Sampling strategy						Dispersion of Pearson coefficient (Pcoeff2)	Fligner–Killeen
	n	mean	median	SD	iqr	cv	χ^2	p value
Audible								
Random	168	−0.0401	−0.0448	0.2255	0.316	5.6203	9.8737	0.00168
Tessellation	153	0.7919	0.8723	0.2528	0.2197	0.3192		
Ultrasound								
Random	48	0.0038	−0.0441	0.2222	0.2340	58.5346	0.4691	0.49342
Tessellation	26	0.8191	0.8656	0.1850	0.1346	0.2259		

Mean, median, standard deviation (SD), interquartile range (IQR), and coefficient of variation (CV) are shown. The Fligner–Killeen test evaluates differences in variability across strategies

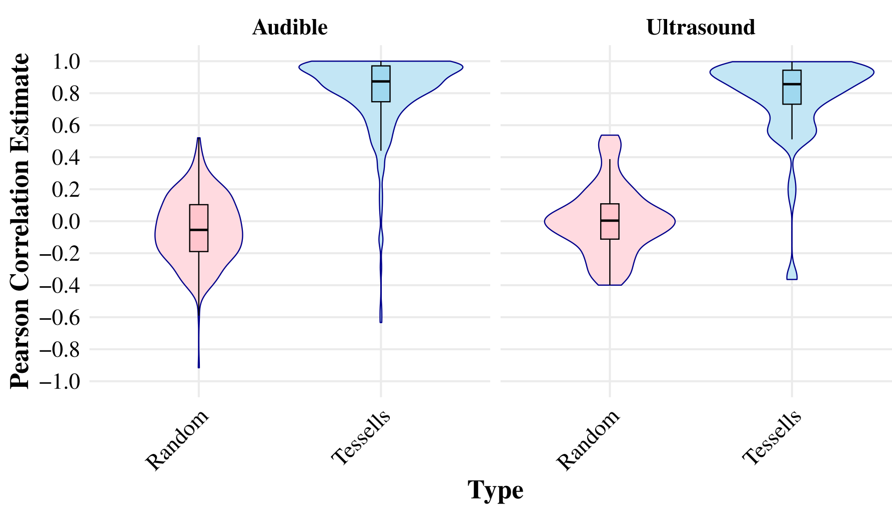

Fig. 4 Distribution of the Pearson correlation coefficient (Pcoeff2) between sample size and sub-sample performance for random (pink) and tessellation-based (blue) designs, in audible and ultrasonic frequencies. The violin plots illustrate the central tendency and dispersion, showing higher consistency and stronger effect size in tessellation strategies

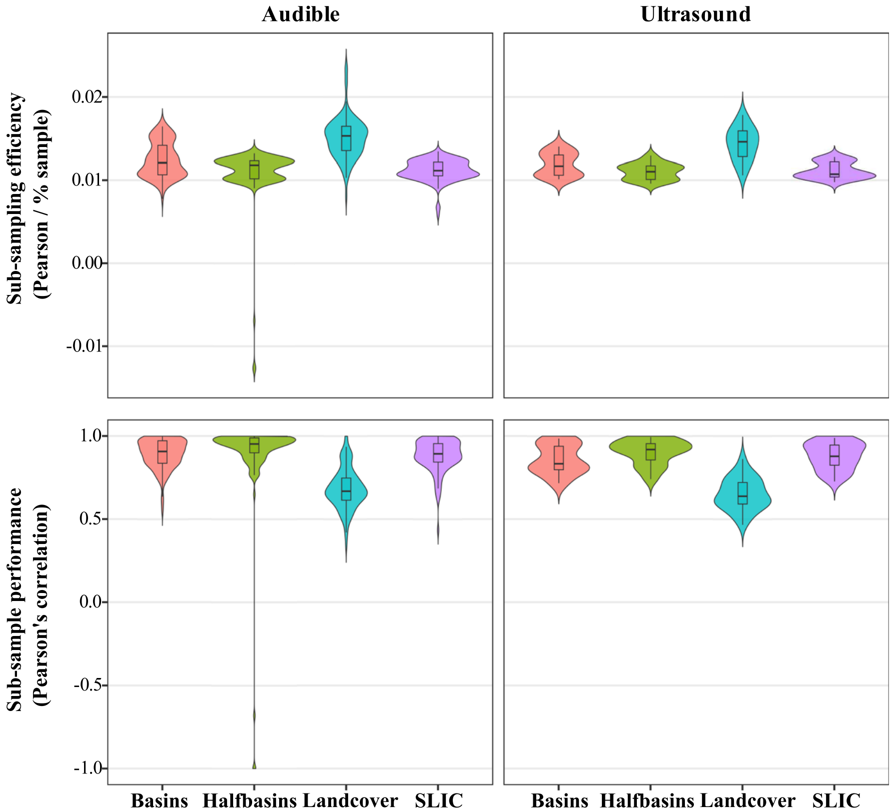

Fig. 5 Sub-sample performance and sampling efficiency across stratified sampling strategies. *Top* sampling efficiency, calculated as sub-sample performance (Pearson's ρ, indicating how well a sub-sample represents the soundscape derived from the full recorder array) divided by sampling proportion. *Bottom* sub-sample performance, measured as the Pearson correlation between each sub-sample's interpolated surface and the full reference grid. Violin and box plots illustrate the distribution of both metrics across landcover-based and tessellation-based strategies

Table 2 Sub-sample evaluation: summary statistics of sub-sample performance and efficiency

Sub-sample	Sub-sample	Mean of performance (Pcoeff1)	Median of performance (Pcoeff1)	SD of performance (Pcoeff1)	Mean of efficiency	Median of efficiency	SD of efficiency	CV of efficiency
Audible	Landcover	0.684	0.6686	0.1225	1.51E−02	1.53E−02	2.43E−03	0.1612
	Basins	0.8924	0.908	0.0873	1.24E−02	1.21E−02	2.08E−03	0.1669
	Halfbasins	0.8904	0.953	0.2901	1.09E−02	1.18E−02	3.59E−03	0.3303
	SLIC	0.8828	0.8939	0.0947	1.12E−02	1.12E−02	1.24E−03	0.1115
Ultrasound	Landcover	0.6511	0.6384	0.0946	1.44E−02	1.46E−02	1.99E−03	0.1382
	Basins	0.8599	0.8341	0.0884	1.19E−02	1.17E−02	1.39E−03	0.1173
	Halfbasins	0.9046	0.9196	0.0740	1.10E−02	1.10E−02	9.63E−04	0.0873
	SLIC	0.8808	0.8789	0.0807	1.11E−02	1.07E−02	9.54E−04	0.0856

Each Sub-sampling design is evaluated by the sub-sample performance (Pcoef1: Pearson correlation with the full raster) and efficiency (sub-sample performance per unit of sampling effort). Reported metrics include the mean and median for performance and efficiency, as well as the standard deviation (SD) and coefficient of variation (CV) for efficiency, to reflect both average performance and its consistency across conditions

contrast, Landcover consistently showed the lowest sub-sample performance (median Pearson < 0.68 in both domains), despite presenting the highest median efficiency (> 0.015 for audible, 0.014 for ultrasound), Landcover also exhibited high variability (CV between 0.16 and 0.13). Basins offered the best overall balance, combining high performance (median Pearson = 0.908 for audible; 0.834 ultrasound) and good efficiency (median = 0.0121, CV = 0.17), performing better than the more precise but less efficient

Halfbasins, and the similarly efficient yet less accurate SLIC across frequency domains (Fig. 5; Table 2; Supplementary Information S6).

Basins showed the highest multivariate structural coherence

We found that the Dimension 1 of the FAMD was primarily associated with efficiency metrics (i.e., sample percent, performance). Therefore, we compare the stratified sampling strategies on Dimensions 2 to 4. We found that Dimension 2 was driven by frequency range, Dimension 3 by interactions of indices and Locality (Locality and Time Period), and Dimension 4 by spatial and temporal stratification (see Supplementary Information S7).

Kruskal–Wallis tests evidence significant differences among Sub-sampling strategies across most FAMD dimensions for both audible and ultrasonic frequencies (all $p < 0.01$; see Supplementary Information S7). The post hoc Dunn tests revealed consistent significance grouping across dimensions. Specifically, we found that the Basins strategy presented the highest structural coherence, frequently occupying group "a". In contrast, Landcover and SLIC exhibited greater variability, often falling into groups "c" or "d", indicating a higher sensitivity to design and environmental variation (Fig. 6).

Landscape heterogeneity was better represented by watershed-based strategies

We found that none of the Kolmogorov–Smirnov tests showed statistically significant differences (all p-values > 0.1); however, the Wasserstein distances revealed marked variation in distributional shape. Specifically, Basins and Halfbasins consistently exhibited the smallest distributional differences from the complete sample (i.e., high representativeness), particularly when considering the selected recorder locations. Unlike the poles of inaccessibility, which represent the geometric center of each tessellation unit, these selected locations correspond to the nearest actual sampling points used to extract landscape proxy values. We consider this distinction as important, because it reflects the transition from theoretical spatial design to real-world landscape variability. For instance, in Andean Urban, Halfbasins (examined) showed the lowest Wasserstein distance (0.0745) and KS statistic (0.0129), indicating excellent alignment with the original landscape structure. Andean Rural

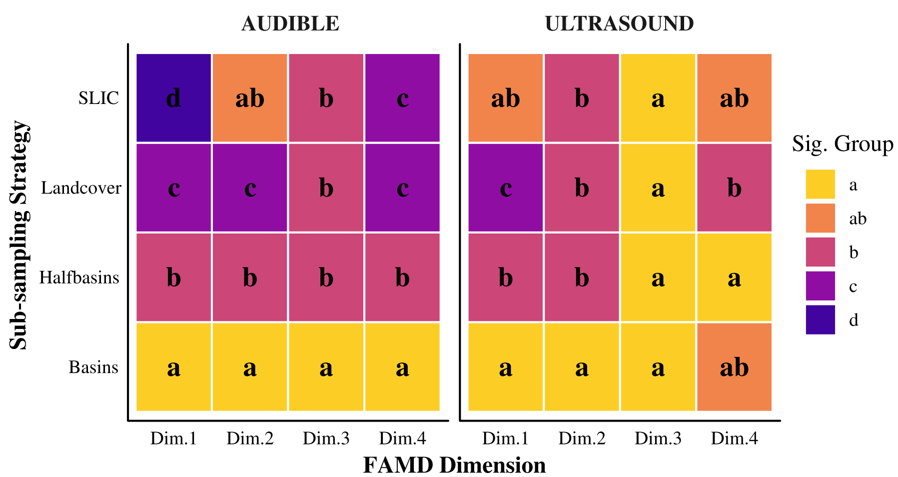

Fig. 6 Comparison of Sub-sampling Strategy across FAMD dimensions based on Dunn's post hoc tests for audible and ultrasound frequencies. Color-coded letters indicate significance groupings for each sampling strategy on Dimensions 1 to 4 derived from the Factorial Analysis of Mixed Data (FAMD). Dimensions 1 to 4 summarize efficiency metrics, frequency range, index–locality–time interactions, and spatial–temporal stratification, respectively. Each letter denotes a statistically distinct cluster ($\alpha = 0.05$), with "a" representing the most cohesive group. The Basins strategy consistently fell within group "a" across dimensions, reflecting higher structural coherence, whereas Landcover and SLIC showed more dispersed groupings (e.g., "c", "d"), suggesting greater variability in response to landscape and design factors

also showed strong alignment for both Basins and Halfbasins strategies.

In contrast, Landcover and SLIC methods often produced larger Wasserstein distances, especially when using Poles as sampling points. For example, in Andean Urban, Landcover (Poles) yielded a Wasserstein distance of 6.36, reflecting substantial divergence from the full distribution. These findings suggest that, although all strategies generally preserve landscape-level patterns, SLIC and Landcover may introduce higher spatial error and variability compared to watershed-based approaches (Table 3).

Discussion

Our findings demonstrate that spatial sampling strongly drives the representativeness of ecoacoustic spatial patterns across heterogeneous landscapes. Stratified tessellation-based approaches, particularly Basins and Halfbasins, consistently outperformed the most common alternatives: random and thematic (i.e., landcover-based) alternatives. Evidence of this can be found in stronger sample size-performance correlations, lower dispersion across sub-samples, and closer alignment with full dataset distributions (Figs. 4, 5, 6). Our results further support an idea often overlooked in large-scale acoustic monitoring:

Table 3 Distributional similarity between complete samples and stratified sub-samples: Kolmogorov–Smirnov and Wasserstein comparisons across localities

Locality	Method	Origin	KS statistic	KS p-value	Wasserstein
Andean Rural	Basins	Examined	0.0942	0.9826	0.8905
		Poles	0.1455	0.7980	1.0103
	Halfbasins	Examined	0.0953	0.9746	0.5412
		Poles	0.1898	0.4651	1.1506
	Landcover	Examined	0.1103	0.9662	1.5187
		Poles	0.1304	0.9240	2.1962
	SLIC	Examined	0.0464	1.0000	1.0884
		Poles	0.1770	0.5516	1.9799
Andean Urban	Basins	Examined	0.0333	1.0000	0.4825
		Poles	0.1244	0.7549	2.0794
	Halfbasins	Examined	0.0129	1.0000	0.0745
		Poles	0.1038	0.8909	1.3909
	Landcover	Examined	0.2705	0.1393	5.9396
		Poles	0.2890	0.1056	6.3556
	SLIC	Examined	0.0548	0.9996	1.3889
		Poles	0.1244	0.7548	2.0804
Plains	Basins	Examined	0.0839	0.9194	4.6849
		Poles	0.1870	0.1395	4.1158
	Halfbasins	Examined	0.0256	1.0000	3.2485
		Poles	0.0752	0.9519	3.0323
	Landcover	Examined	0.1793	0.2869	5.984
		Poles	0.1628	0.4134	6.1022
	SLIC	Examined	0.0539	0.9976	3.382
		Poles	0.1693	0.1698	4.9078

Comparison of each stratified sampling strategy's ability to replicate the distribution of the soundscape derived from the full landscape sample, using Kolmogorov–Smirnov (KS) statistics and Wasserstein distances. Lower KS values indicate higher overlap between empirical distributions, while lower Wasserstein distances reflect minimal divergence in shape and central tendency. Results are shown for two types of sampling point origin, "Poles" (pole of inaccessibility) and "Examined" (nearest original recorder), across three localities. While no KS comparisons reached statistical significance (all $p > 0.1$), substantial differences in Wasserstein distances suggest that watershed-based methods (Basins, Halfbasins) better capture landscape heterogeneity than Landcover or SLIC, particularly when using the examined points not only sample quantity matters, but also the spatial logic (Wang et al. 2012).

One reason tessellation-based strategies may have outperformed other designs is their ability to adapt sampling units to the physical heterogeneity of the landscape. In our case, the watershed-based approaches (Basins and Halfbasins) applied the r.watershed algorithm to a continuous landscape proxy derived from satellite imagery. Rather than delineating real hydrological watersheds, this procedure partitions the landscape into spatially coherent units that follow gradients in the input data. By treating pixel values as a virtual surface, the algorithm generates irregular regions that are internally more homogeneous with respect to the proxy used, which may better preserve the landscape heterogeneity that researchers often aim to represent when deploying acoustic recorders. This does not imply that such units necessarily contain homogeneous soundscapes, but it does provide a landscape-informed basis for sampling design. Other landscape units could also be appropriate depending on the study objective, but watershed-based segmentation may be especially useful when the goal is to capture continuous landscape gradients while avoiding rigid boundaries, in line with spatial sampling principles that emphasize spatial autocorrelation and the avoidance of clustered sampling points (Wang et al. 2012; Sun 2015).

Watershed segmentation reflects key spatial sampling principles by interpreting pixel values as elevation to generate homogeneity-based, adaptively shaped segments (Wang et al. 2012). This method leverages spatial auto correlation to ensure uniform coverage, reduce analytical uncertainty, and prevent point clustering, achieving effects similar to those of precise sampling. Although the SLIC algorithm is based on similar principles, it is less adaptive and relies on rigid, axis-aligned segmentation, especially in the configuration used here (Neubert and Protzel 2014; Nowosad and Stepinski 2021). These limitations may explain its lower performance in representing soundscape indicators and landscape heterogeneity.

Both Landcover and Random sampling designs showed the lowest performance among the evaluated methods. In the case of Landcover, it is important to note that the sampling strategy was derived from a specific landscape proxy, constructed through a particular segmentation process. While this approach served our analysis, it represents only one possible interpretation of landscape heterogeneity under the label "landcover." Therefore, the results may reflect the limitations of this specific implementation and do not necessarily generalize to all landcover-based sampling frameworks.

More broadly, we point out that both discrete and continuous proxies represent aggregations of ecotopes, but they differ in how spatial heterogeneity is expressed. Discrete proxies define ecotopes as landcover patches with predefined boundaries and variable sizes, whereas continuous proxies represent ecotopes as equally sized raster units, whose resolution depends on the pixel size. Our results are consistent with the expectation that gradient-based, continuous proxies may better capture spatial heterogeneity relevant for sampling design, particularly for methods such as watershed segmentation. However, we emphasize that this interpretation is inferential rather than directly tested here, as resolution effects were not explicitly manipulated in our analyses.

While several studies have shown that soundscape patterns exhibit spatial associations with landscape composition and configuration, these associations are neither consistent nor strictly linear (Fuller et al. 2015; Scarpelli et al. 2021). Recent work also suggests that acoustic patterns can display emergent properties that only partially correspond to the physical landscape, highlighting the need for more nuanced approaches that incorporate temporal variability and scale-dependent decoupling, that is, changes in landscape–soundscape correspondence across frequency bands and temporal windows (Guerrero et al. 2025; Rendón et al. 2025). Additionally, it is important to note that the soundscape indices used here predominantly reflect biophonic activity within the audible spectrum, which in tropical and Andean ecosystems is largely driven by birds, insects, and to a lesser extent amphibians. Therefore, the interpolated spatial patterns represent aggregated acoustic activity from multiple sources (biological and non-biological) rather than taxon-specific ecological processes.

Because our aim was to evaluate the spatial representativeness of sub-sampling strategies, rather than to infer specific community composition, this level of aggregation is appropriate for assessing how

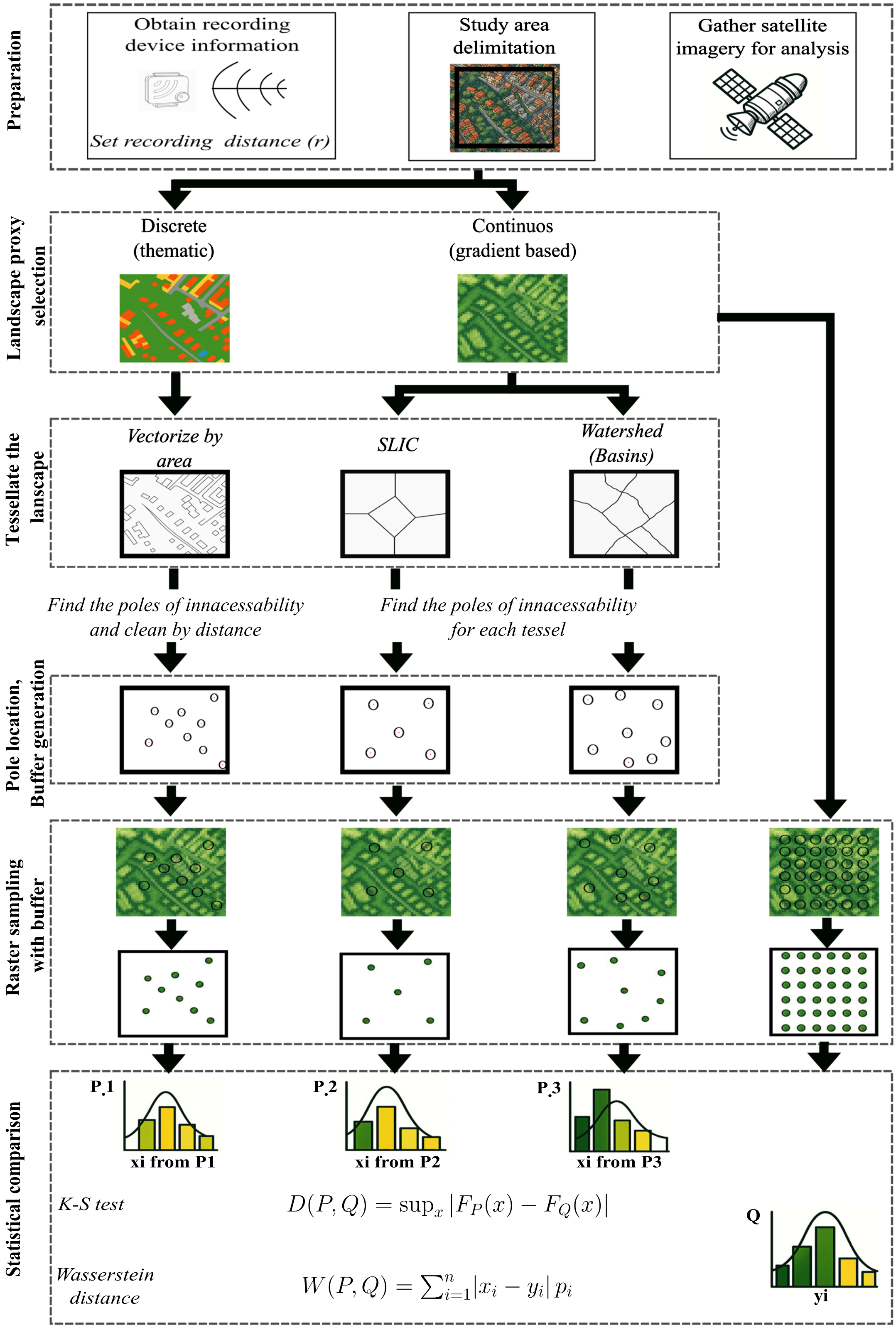
Preparation
Obtain recording device information
Set recording distance (r)
Study area delimitation
Gather satellite imagery for analysis
Landscape proxy selection
Discrete (thematic)
Continuos (gradient based)
Tessellate the lanscape
Vectorize by area
SLIC
Watershed (Basins)
Find the poles of innacessability and clean by distance
Find the poles of innacessability for each tessel
Pole location, Buffer generation
Raster sampling with buffer
Statistical comparison
P.1
xi from P1
P.2
xi from P2
P.3
xi from P3
K-S test
$D(P,Q) = \sup_x |F_P(x) - F_Q(x)|$
Wasserstein distance
$W(P,Q) = \sum_{i=1}^{n} |x_i - y_i| \, p_i$
Q
yi

◂**Fig. 7** Proposed workflow for spatial sampling design in ecoacoustic studies. The workflow integrates landscape proxy selection, tessellation, central point extraction, and statistical validation. It compares each Sub-sampling strategy against a reference full-grid scenario using both the Kolmogorov–Smirnov test (for statistical similarity) and the Wasserstein distance (for distributional divergence). Landscape proxies can be discrete (e.g., landcover) or continuous (e.g., vegetation gradients), and tessellation methods include vector-based segmentation, SLIC, and Watershed (Basins). The complete methodological protocol and decision rules are described in Supplementary Information S10 (Colab file). The full-grid scenario shown in the workflow represents an idealized reference used exclusively for comparative evaluation and is not intended as a recommended sampling scheme for practical implementation

well landscape-informed sampling designs capture broad spatial patterns in acoustic activity. Nonetheless, this implies that the ecological meaning of the soundscape surface depends on both biotic and non-biotic sound dominating the analyzed frequency range. Importantly, we observed highly consistent patterns between audible and ultrasonic analyses, indicating that the relative performance of spatial sampling strategies is robust across acoustic frequency domains. In ecosystems where ultrasonic taxa (e.g. bats or orthopterans) or low-frequency species play a dominant role, different frequency bands may reveal distinct spatial structures. Thus, while our methodological approach is taxon-independent and can be applied to any acoustic metric or frequency band, the ecological interpretation of representativeness must be contextualized by the biological groups contributing most strongly to the soundscape within the chosen spectral window.

Our findings are not just consistent with previous interpretations of landscape representation, but also reinforce a key principle often overlooked in large-scale acoustic monitoring: spatial logic is as critical as sample size (Wang et al. 2012). Random sampling, regardless of size, yielded unstable correlations and unpredictable performance. This illustrates that even large sampling efforts, when applied randomly, do not guarantee representativeness (Nuñez-Penichet et al. 2022). In fact, random designs may create a false sense of coverage while undermining the reliability of ecological inferences.

Another important consideration is that our analysis focused exclusively on soundscape indices. Future research should explore how spatially optimized sampling designs influence the detection and interpretation of ecologically meaningful patterns, such as biodiversity or species-specific acoustic signals. Further studies could also assess how different segmentation approaches, when applied across diverse ecosystems and remote sensing inputs, affect sampling efficiency for other ground-based monitoring systems. Additionally, although we used a fixed radius of 200 m (based on Bicudo et al. 2023) to define the tessellation scale, this value should not be interpreted as a strict estimate of biological detection distance. Instead, it represents an operational spacing threshold selected to maintain spatial independence among recorders and to stabilize variogram estimation during interpolation, used here to compare between different sampling sizes. We also kept a constant radius to ensure methodological consistency; however, this methodology is flexible and can accommodate different radii in future applications depending on habitat structure, taxa of interest, or specific monitoring objectives. Thus, the scale of A_i should be understood as a spatial design parameter, and not necessarily as a proxy for acoustic propagation or perceptual range.

Finally, to consolidate our findings and support their practical application, we developed a structured workflow for ecoacoustic sampling design based on landscape heterogeneity. We remark that this workflow is not intended to prescribe exhaustive grid-based sampling in real-world applications. Instead, the full-grid scenario used here represents an idealized reference condition, employed solely as a comparative benchmark to evaluate how well alternative sub-sampling designs preserve spatial patterns. By using this reference as a common baseline, the framework allows researchers to identify sampling strategies that most closely approximate the spatial structure of the landscape while substantially reducing sampling effort. The framework integrates landscape proxy selection, tessellation, sampling point placement, and statistical validation to guide a priori sampling design decisions, rather than to replicate complete sampling campaigns. In this sense, the workflow offers a scalable tool for optimizing spatial sampling in ecoacoustics and other spatially explicit ecological studies (Fig. 7). The detailed procedure is available in Supplementary Information S9.

While our workflow focuses on maximizing the structural representation of the landscape heterogeneity through segmentation and spatial logic, alternative frameworks such as Generalized Random Tessellation Stratified (GRTS) sampling have proven effective in population-level ecological monitoring (Stevens and Olsen 2004; Kermorvant et al. 2019). However, GRTS is designed primarily for probabilistic inference and population representativeness, whereas our approach is tailored for landscape-based applications where the goal is to preserve spatial patterns with minimal sampling effort. In this context, our method emphasizes how to tessellate the landscape meaningfully, providing a structural foundation that can be paired with various sampling schemes depending on the research question. For instance, while our workflow uses the Kolmogorov–Smirnov and Wasserstein distance to quantify structural alignment, users seeking statistical inference could adapt the resulting tessellations within a GRTS framework or other probability-based strategies.

Conclusions

The aim of our study was to examine how spatial sampling design influences the representativeness of soundscape information in ecoacoustic research across heterogeneous landscapes. Specifically, we evaluated how different spatial sampling strategies affect data reliability under varied environmental conditions. This allowed us to show that data reliability is not an inherent property of the sensors, but a product of the spatial logic applied to their deployment.

Our study has identified stratified tessellation-based methods, particularly Basins and Halfbasins, as consistently outperforming random and thematic approaches. The results of this investigation show that these spatially structured designs yielded higher precision, lower dispersion, and stronger correlations with sampling effort. The most important finding from this study is that sampling performance is not solely dependent on sample size, but critically on the spatial configuration of the sampling scheme. In contrast, Landcover and Random designs resulted in greater variability, reduced structural alignment, and higher spatial error.

Based on the results of this study, we propose a "Workflow for Sampling Design in Ecoacoustic Studies" that aligns with the principle of prioritizing spatial logic in ecological monitoring. Our approach provides a structured method for improving the representativeness of ecoacoustic data in heterogeneous landscapes. These findings have significant implications for the development of soundscape-based monitoring strategies and may be particularly relevant to researchers in conservation, biodiversity assessment, and spatial ecology.

In conclusion, spatially explicit and ecologically informed sampling designs offer a powerful foundation for advancing ecoacoustic research. By aligning sampling frameworks with the underlying structure of the landscape, researchers can improve data reliability, economize resources, reduce spatial bias, and support more effective ecological inference in different environments.

Acknowledgements We thank Paubla Otálvaro, Santiago Aricapa, Jovino Morales, and all the people from the communities of "Mano de Sol" and the localities of San Lorenzo, El Popo, and San Miguel in the Municipality of Alejandría (Antioquia, Colombia) for their invaluable aid during fieldwork. We thank Diego González and all the staff of the "Rey Zamuro" Reserve (Meta, Colombia). We also thank the Mayor's Office and the Department of Environment of the Municipality of La Estrella (Antioquia, Colombia) for their logistical and financial support during the field phase.

The authors V. Martínez-Arias and C. Paniagua-Villada wish to express their gratitude to Dr. Juan D. Gómez González for his "Scientific Writing in English" course in the Biology Graduate Program at the University of Antioquia.

Finally, we thank the Editor and the three anonymous reviewers for their time, expertise, and constructive feedback, which greatly strengthened the conceptual framing, methodological clarity, and interpretation of our results.

Author contributions All authors contributed to the study conception and design. Material preparation, data collection and analysis were performed by Victor M. Martinez-Arias, Carolina Paniagua-Villada, María J. Guerrero, and Juan Daza. The first draft of the manuscript was written by Victor M. Martinez-Arias, and all authors commented on previous versions of the manuscript. All authors read and approved the final manuscript.

Funding Open Access funding provided by Colombia Consortium. This research was funded by the Research Program "Biodiversity Conservation using Artificial Intelligence" with code 111585269779 of the Colombian National Program of Science, Technology, and Innovation in Environment, Biodiversity and Habitat.

Data availability Supplementary Information including codes, cartography, workflow, and datasets, are available in Martinez-Arias et al. (2025). Supplementary information for:

A workflow to optimize spatial sampling in ecoacoustic studies (Data set). Zenodo. https://doi.org/10.5281/zenodo.20078843.

Declarations

Conflict of interest The authors have no relevant financial or non-financial interests to disclose.

References

Abdi H, Williams LJ (2010) Principal component analysis. WIREs Comput Stat 2:433–459

Abrahams C, Desjonquères C, Greenhalgh J (2021) Pond acoustic sampling scheme: a draft protocol for rapid acoustic data collection in small waterbodies. Ecol Evol 11:7532–7543

Achanta R, Shaji A, Smith K, Lucchi A, Fua P, Süsstrunk S (2012) SLIC superpixels compared to state-of-the-art superpixel methods. IEEE Trans Pattern Anal Mach Intell 34:2274–2282

Alcocer I, Lima H, Sugai LSM, Llusia D (2022) Acoustic indices as proxies for biodiversity: a meta-analysis. Biol Rev 97:2209–2236

Ali A, De Bie CAJM, Skidmore AK, Scarrott RG, Lymberakis P. (2014) Mapping the heterogeneity of natural and semi-natural landscapes. Int J Appl Earth Obs Geoinf 26:176–183

Amelia R, Julianti E, Guskarnali (2023) Implementation of Inverse Distance Weighting (IDW) and Kriging method for distribution pattern humidity and temperature data on weather changes in the Bangka Islands. IOP Conf Ser Earth Environ Sci 1267:012091

Bedoya C, Isaza C, Daza JM, López JD (2017) Automatic identification of rainfall in acoustic recordings. Ecol Indic 75:95–100

Bicudo T, Llusia D, Anciães M, Gil D (2023) Poor performance of acoustic indices as proxies for bird diversity in a fragmented Amazonian landscape. Ecol Inform 77:102241

Boelman NT, Asner GP, Hart PJ, Martin RE (2007) Multitrophic invasion resistance in Hawaii: bioacoustics, field surveys, and airborne remote sensing. Ecol Appl 17:2137–2144

Borcard D, Gillet F, Legendre P (2011) Numerical ecology with R. Springer, New York

Bradfer-Lawrence T, Duthie B, Abrahams C, Adam M, Barnett RJ, Beeston A, Darby J, Dell B, Gardner N, Gasc A, Heat B, Howells N, Janson M, Kyoseva M-V, Luypaert T. Ross SRP-J, Sethi S, Smyth S, Waddell E, Froidevaux JSP (2025) The acoustic index user's guide: a practical manual for defining, generating and understanding current and future acoustic indices. Methods Ecol Evol 16:1040–1050

Cansler CA, McKenzie D (2012) How robust are burn severity indices when applied in a new region? Evaluation of alternate field-based and remote-sensing methods. Remote Sens 4:456–483

Chen X, Sarkar SK (2020) On Benjamini-Hochberg procedure applied to mid p-values. J Stat Plan Inference 205:34–45

Farina A (2022) Principles for landscape conservation, management, and design. In: Principles and methods in landscape ecology. Springer, Cham

Farina A, Li P (2022) Methods in ecoacoustics: the acoustic complexity indices. Springer, Cham

Farina A, Mullet TC, Bazarbayeva TA, Tazhibayeva T, Polyakova S, Li P (2023) Sonotopes reveal dynamic spatio-temporal patterns in a rural landscape of Northern Italy. Front Ecol Evol 11:1205272

Farina A, Krause B, Mullet TC (2024) An exploration of ecoacoustics and its applications in conservation ecology. BioSystems 245:105296

Fortin MJ, Drapeau P, Legendre P (1989) Spatial autocorrelation and sampling design in plant ecology. Vegetatio 83:209–222

Francis RA, Millington JDA, Perry GLW, Minor ES (eds) (2022) The Routledge handbook of landscape ecology. Routledge, Taylor & Francis Group; London, New York

Fuller S, Axel AC, Tucker D, Gage SH (2015) Connecting soundscape to landscape: which acoustic index best describes landscape configuration? Ecol Indic 58:207–215

Gibb R, Browning E, Glover-Kapfer P, Jones KE (2019) Emerging opportunities and challenges for passive acoustics in ecological assessment and monitoring. Methods Ecol Evol 10(2):169–185

Gillies S (2013) The Shapely user manual

Google Earth Engine (2023a) ee.ImageCollection.errorMatrix

Google Earth Engine (2023b) Ee.Classifier. SmileRandomForest

Gorelick N, Hancher M, Dixon M, Ilyushchenko M, Thau D, Moore R (2017) Google Earth Engine: planetary-scale geospatial analysis for everyone. Remote Sens Environ. https://doi.org/10.1016/j.rse.2017.06.031

Guerrero MJ, Sánchez-Giraldo C, Uribe CA, Martínez-Arias VM, Isaza C (2025) Graphical representation of landscape heterogeneity identification through unsupervised acoustic analysis. Methods Ecol Evol 16(6):1255–1272

Hejmanowska B, Kramarczyk P, Głowienka E, Mikrut S (2021) Reliable crops classification using limited number of Sentinel-2 and Sentinel-1 images. Remote Sens 13:3176

Hong S, Kim S, Cho KH, Kim JE, Kang S, Lee D (2004) Ecotope mapping for landscape ecological assessment of habitat and ecosystem. Ecol Res 19:131–139

Kassambara A (2017) Practical guide to principal component methods in R, Edition 1. CreateSpace Independent Publishing Platform

Kassambara A (2019) rstatix: Pipe-friendly framework for basic statistical tests. 0.7.2

Kassambara A (2023) ggpubr: "ggplot2" based publication ready plots

Kasten EP, Gage SH, Fox J, Joo W (2012) The remote environmental assessment laboratory's acoustic library: an archive for studying soundscape ecology. Ecol Inform 12:50–67

Kemp J, Azofeifa-Solano JC, Barneche DR, Brooker R, Arévalo JE, Erbe C, Parsons M (2025) Impact of acoustic index parameters on soundscape comparisons. Methods Ecol Evol 16:872–885

Kermorvant C, D'Amico F, Bru N, Caill-Milly N, Robertson B (2019) Spatially balanced sampling designs for environmental surveys. Environ Monit Assess 191:524

Kerr JT, Ostrovsky M (2003) From space to species: ecological applications for remote sensing. Trends Ecol Evol 18:299–305

Kriegler F, Malila W, Nalepka R, Richardson W (1969) Preprocessing transformations and their effects on multispectral recognition. Remote Sens Environ VI:97

Luna-Naranjo D, Martinez-Vargas JD, Sánchez-Giraldo C, Daza JM, López JD (2024) Quantifying and mitigating recorder-induced variability in ecological acoustic indices. Ecol Inform 82:102668

Lymburner L, Beggs PJ, Jacobson CR (2000) Estimation of canopy-average surface-specific leaf area using Landsat™ data. Photogramm Eng Remote Sens 66:183–192

Metcalf O, Abrahams C, Ashington B, Baker E, Bradfer-Lawrence T, Browning E, Carruthers-Jones J, Darby J, Dick J, Eldridge A, Elliott D, Heath B, howden-Leach P, Johnston A, Lees A, Meyer C, Ruiz Arana U, Smyth S (2023) Good practice guidelines for long-term ecoacoustic monitoring in the UK. The UK Acoustics Network - Technical Report

Milne BT (1991) Heterogeneity as a multiscale characteristic of landscapes. In: Kolasa J, Pickett STA (eds) Ecological heterogeneity. Springer, New York, pp 69–84

Mishra V, Kumar S, Singh C (2014) Implementation and comparison of image fusion using discrete wavelet transform and principal component analysis. Int J Comput Sci Eng 2(3):174–181

Neubert P, Protzel P (2014) Compact watershed and preemptive SLIC: on improving trade-offs of superpixel segmentation algorithms. In: 2014 22nd International conference on pattern recognition, 2014. IEEE, Stockholm, pp 996–1001

Nowosad J, Stepinski T (2021) Generalizing the simple linear iterative clustering (SLIC) superpixels. In: GIScience 2021 short paper proceedings 11th international conference on geographic information science, 27–30 September 2021, Poznań (online). https://doi.org/10.25436/E2QP4R

Nuñez-Penichet C, Cobos ME, Soberón J, Gueta T, Barve N, Barve V, Navarro-Sigüenza AG, Peterson AT (2022) Selection of sampling sites for biodiversity inventory: effects of environmental and geographical considerations. Methods Ecol Evol 13:1595–1607

Ogle D, Doll J, Wheeler A, Dinno A (2025) FSA: simple fisheries stock assessment methods_. R package version 0.9.6

Palomino N, Hilares NG (2011) Implementación del algoritmo Watershed para el análisis de imágenes médicas. RISI 8:67–74

R Core Team (2024) R: a language and environment for statistical computing. R Foundation for Statistical Computing, Vienna

Radoux J, Bourdouxhe A, Coos W, Dufrêne M, Defourny P (2019) Improving ecotope segmentation by combining topographic and spectral data. Remote Sens 11:1–15

Ramdas A, Trillos N, Cuturi M (2017) On Wasserstein two-sample testing and related families of nonparametric tests. Entropy Basel 19:47

Rendon N, Rodríguez-Buritica S, Sanchez-Giraldo C et al (2022) Automatic acoustic heterogeneity identification in transformed landscapes from Colombian tropical dry forests. Ecol Indic 140:109017

Rendon N, Guerrero MJ, Sánchez-Giraldo C, Martinez-Arias VM, Paniagua-Villada C, Bouwmans T, Daza J, Isaza C (2025) Letting ecosystems speak for themselves: an unsupervised methodology for mapping landscape acoustic heterogeneity. Environ Model Softw 187:106373

Ross SRPJ, O'Connell DP, Deichmann, Desjonquères C, Gasc A, Phillips JN, Sethi SS, Wood CM, Burivalova Z (2023) Passive acoustic monitoring provides a fresh perspective on fundamental ecological questions. Funct Ecol 37:959–975

Sánchez-Giraldo C, Correa Ayram C, Daza JM (2021) Environmental sound as a mirror of landscape ecological integrity in monitoring programs. Perspect Ecol Conserv 19:319–328

Sarkar S, Kim C, Basu A (1999) Tests for homogeneity of variances using robust weighted likelihood estimates. Biom J 41:857–871

Scarpelli MD, Ribeiro MC, Teixeira CP (2021) What does Atlantic Forest soundscapes can tell us about landscape? Ecol Indic 121:107050

Stevens DL, Olsen AR (2004) Spatially balanced sampling of natural resources. J Am Stat Assoc 99:262–278

Sugai LS, Silva TSF, Ribeiro JW Jr, Llusia D (2019) Terrestrial passive acoustic monitoring: review and perspectives. Bioscience 69:15–25

Sun H (2015) Watershed image segmentation algorithm base on particle swarm and region growing. In: Proceedings of 2015 international conference on intelligent computing and Internet of Things, 2015. IEEE, Harbin, pp 51–54

Ulloa JS, Haupert S, Latorre JF, Aubin T, Sueur, J (2021) Scikit-maad: an open-source and modular toolbox for quantitative soundscape analysis in Python. Methods Ecol Evol 12:2334–2340

Wang J-F, Stein A, Gao B-B, Ge Y (2012) A review of spatial sampling. Spat Stat 2:1–14

Wickham H (2011) ggplot2. WIREs Comput Stat 3:180–185

Wickham H, François R, Henry L et al (2014) dplyr: a grammar of data manipulation. 1.1.4

Xu H (2006) Modification of normalized difference water index (NDWI) to enhance open water features in remotely sensed imagery. Int J Remote Sens 27:3025–3033

Zarco-Perello S, Simões N (2017) Ordinary kriging vs inverse distance weighting: spatial interpolation of the sessile community of Madagascar Reef, Gulf of Mexico. PeerJ 5:e4078